LETTER

doi:10.1038/nature13267

Cyclin D1–Cdk4 controls glucose metabolism independently of cell cycle progression

Yoonjin Lee[1,2,3], John E. Dominy[1,2], Yoon Jong Choi[1,4], Michael Jurczak[5], Nicola Tolliday[6], Joao Paulo Camporez[5], Helen Chim[1,2], Ji-Hong Lim[1,2], Hai-Bin Ruan[5], Xiaoyong Yang[5], Francisca Vazquez[1,2], Piotr Sicinski[1,4], Gerald I. Shulman[5] & Pere Puigserver[1,2]

Insulin constitutes a principal evolutionarily conserved hormonal axis for maintaining glucose homeostasis[1–3]; dysregulation of this axis causes diabetes[2,4]. PGC-1α (peroxisome-proliferator-activated receptor-γ coactivator-1α) links insulin signalling to the expression of glucose and lipid metabolic genes[5–7]. The histone acetyltransferase GCN5 (general control non-repressed protein 5) acetylates PGC-1α and suppresses its transcriptional activity, whereas sirtuin 1 deacetylates and activates PGC-1α[8,9]. Although insulin is a mitogenic signal in proliferative cells[10,11], whether components of the cell cycle machinery contribute to its metabolic action is poorly understood. Here we report that in mice insulin activates cyclin D1–cyclin-dependent kinase 4 (Cdk4), which, in turn, increases GCN5 acetyltransferase activity and suppresses hepatic glucose production independently of cell cycle progression. Through a cell-based high-throughput chemical screen, we identify a Cdk4 inhibitor that potently decreases PGC-1α acetylation. Insulin/GSK-3β (glycogen synthase kinase 3-beta) signalling induces cyclin D1 protein stability by sequestering cyclin D1 in the nucleus. In parallel, dietary amino acids increase hepatic cyclin D1 messenger RNA transcripts. Activated cyclin D1–Cdk4 kinase phosphorylates and activates GCN5, which then acetylates and inhibits PGC-1α activity on gluconeogenic genes. Loss of hepatic cyclin D1 results in increased gluconeogenesis and hyperglycaemia. In diabetic models, cyclin D1–Cdk4 is chronically elevated and refractory to fasting/feeding transitions; nevertheless further activation of this kinase normalizes glycaemia. Our findings show that insulin uses components of the cell cycle machinery in post-mitotic cells to control glucose homeostasis independently of cell division.

To discover new factors that can regulate PGC-1α activity through its acetylation status, a high-throughput enzyme-linked immunoassay was designed to monitor specifically and quantitatively the amount of PGC-1α acetylation in U-2OS cells (Extended Data Fig. 1a). A library of 1,600 compounds, including bioactive and natural compounds, was screened (Fig. 1a). Interestingly, the compound with the highest *z* score for PGC-1α deacetylation was fascaplysin, a known Cdk4 inhibitor[12] (Extended Data Fig. 1b). Cdk4 regulates G1 to S phase transition and its kinase activity is dependent on its binding to one of the three D-type cyclins including cyclin D1 (ref. 13). We therefore investigated the effect of this cell cycle complex on PGC-1α acetylation and function, in connection with nutrient and insulin metabolic actions.

First, we calculated a half-maximum inhibitory concentration (IC_{50}) of 0.7 μM for fascaplysin-induced PGC-1α deaceylation, which is similar to its IC_{50} for Cdk4 inhibition (Extended Data Fig. 2a). Fascaplysin-induced PGC-1α deacetylation overlapped with retinoblastoma protein (Rb) dephosphorylation, a well-characterized Cdk4 substrate[14] (Fig. 1b). PD 0332991, the most specific Cdk4 inhibitor available[15], led to a similar decrease of PGC-1α acetylation (Fig. 1c and Extended Data Fig. 2b). Furthermore, Cdk4 depletion through transient short hairpin RNA (shRNA) transfection had the same effect as chemical inhibitors, confirming that Cdk4 activity controls PGC-1α acetylation levels (Fig. 1d and Extended Data Fig. 2c).

Because Cdk4 inhibitor-induced PGC-1α deacetylation was not affected when sirtuin 1 (SIRT1) or HDAC class I/II were inhibited (Extended Data Fig. 2d), we tested whether cyclin D1–Cdk4 regulates PGC-1α acetylation through GCN5, the principal PGC-1α acetyltransferase. Indeed, knockdown of *Gcn5* significantly blunted fascaplysin-induced PGC-1α deacetylation (Fig. 1e). In contrast, PCAF-mediated acetylation was not affected by fascaplysin, further suggesting that Cdk4 inhibition modulates PGC-1α acetylation through GCN5 (Extended Data Fig. 2e). *In vitro* catalytic activity of GCN5 immunoprecipitated from cells treated with fascaplysin was reduced by 50% relative to vehicle control (Fig. 1f). We observed physical interaction between ectopically expressed or endogenous Cdk4 and GCN5, suggesting that Cdk4 could regulate GCN5 activity by direct phosphorylation (Fig. 1g and Extended Data Fig. 2f). Cyclin D1–Cdk4 kinase directly phosphorylated GCN5 *in vitro* and its phosphorylation was inhibited by fascaplysin (Fig. 1h and Extended Data Fig. 2g). Systematic mutagenesis showed two phosphorylation sites, T272 and S372, located in the conserved PCAF domain of GCN5. Alanine substitutions of these two sites ('GCN5 AA') ablated GCN5 phosphorylation by cyclin D1–Cdk4 *in vitro*, and reduced PGC-1α acetylation (Fig. 1i, 1j and Extended Data Fig. 2h, i). Compared with GCN5 wild type, *in vitro* catalytic activity of GCN5 AA was decreased, but remained insensitive to fascaplysin (Fig. 1k). Cdk4 phosphorylation on GCN5 augmented acetyltransferase catalytic activity by increasing maximal velocity (V_{max}), whereas the Michaelis–Menten constant (K_m) for acetyl-CoA binding was unaffected (Fig. 1k). Because GCN5 functions as a complex with subunits important for its activity[16], its phosphorylation by Cdk4 could modulate interaction between GCN5 and subunits. We found one subunit, PAF65-β, interacting less with GCN5 AA compared with GCN5 wild type, when tested with modestly overexpressed GCN5, where PGC-1α acetylation was not saturated (Extended Data Fig. 2j, k). Taken together, these results indicate that cyclin D1–Cdk4 regulates PGC-1α acetylation through the direct phosphorylation and activation of GCN5 acetyltransferase activity.

Because PGC-1α acetylation is tightly linked with its co-transcriptional activity[8,9,17], we investigated whether cyclin D1–Cdk4 could modulate the gluconeogenic target genes of PGC-1α. To study cyclin D1–Cdk4 kinase effects in a PGC-1α mediated manner, we induced PGC-1α in primary hepatocytes by adenoviral overexpression or forskolin addition (Extended Data Fig. 3a). In primary hepatocytes, chemical inhibition of Cdk4 significantly increased gluconeogenic genes and glucose production, consistent with reduced PGC-1α acetylation (Fig. 2a–c and Extended Data Fig. 3b). Cdk4 depletion produced similar effects (Fig. 2d–f and Extended Data Fig. 3c). Conversely, induction of CKD4 activity by cyclin D1 wild-type overexpression or cyclin D1 T286A mutant, a hyperactive mutant allele spared from proteasomal degradation[18], but not cyclin D1 K112E (a mutant that cannot activate Cdk4 kinase activity[19]), suppressed

[1]Department of Cancer Biology, Dana-Farber Cancer Institute, Boston, Massachusetts 02115, USA. [2]Department of Cell Biology, Harvard Medical School, Boston, Massachusetts 02115, USA. [3]Department of Chemistry and Chemical Biology, Harvard University, Cambridge, Massachusetts 02138, USA. [4]Department of Genetics, Harvard Medical School, Boston, Massachusetts 02115, USA. [5]Yale's Mouse Metabolic Phenotyping Center and Departments of Internal Medicine and Cellular and Molecular Physiology, Yale University School of Medicine, New Haven, Connecticut 06510, USA. [6]Chemical Biology Platform, Broad Institute of Harvard and MIT, 7 Cambridge Center, Cambridge, Massachusetts 02141, USA.

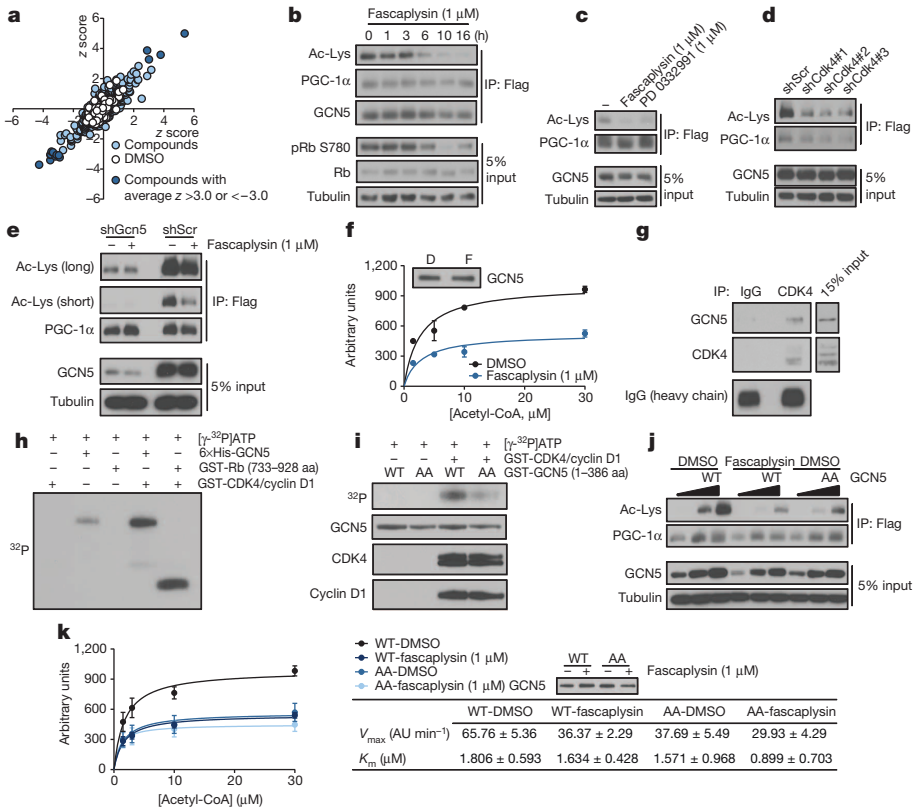

	WT-DMSO	WT-fascaplysin	AA-DMSO	AA-fascaplysin
V_{max} (AU min^{-1})	65.76 ± 5.36	36.37 ± 2.29	37.69 ± 5.49	29.93 ± 4.29
K_m (μM)	1.806 ± 0.593	1.634 ± 0.428	1.571 ± 0.968	0.899 ± 0.703

Figure 1 | Cyclin D1–Cdk4 modulates PGC-1α acetylation through GCN5. **a**, Scatter plot of chemicals plotted with first test *z* scores on the *x* axis and repeated test scores on the *y* axis. DMSO, dimethylsulphoxide. **b**, Fascaplysin reduces PGC-1α acetylation and Rb phoshorylation. **c**, Fascaplysin and PD 0332991 treatments decrease PGC-1α acetylation. **d**, *Cdk4* knockdown causes PGC-1α deacetylation. **e**, *Gcn5* knockdown blunts fascaplysin-mediated PGC-1α deacetylation. **f**, GCN5 acetyltransferase activity is reduced upon fascaplysin treatment ($n = 2$, technical replicates, mean ± s.e.m., *y* axis represents florescence generated for 15 min from the assay). D, DMSO; F, fascaplysin. **g**, Endogenous GCN5 and Cdk4 interact. **h**, Cyclin D1–Cdk4 kinase phosphorylates GCN5 *in vitro*. aa, amino acids. **i**, GCN5 T272A/S372A (AA) phosphorylation by cyclin D1–Cdk4 kinase is diminished compared with GCN5 wild type (WT). **j**, GCN5 T272A/S372A shows decreased acetyltransferase capacity. **k**, GCN5 T272A/S372A has decreased acetyltransferase activity and insensitivity to fascaplysin treatment. Kinetic constants were calculated by the Michaelis–Menten equation ($n = 4$, two biological replicates assayed in duplicate; AU/min, arbitrary units per minute, mean ± s.e.m., *y* axis represents florescence generated for 15 min from the assay). U-2OS cells were used for these experiments.

gluconeogenic genes and glucose production, corresponding with PGC-1α acetylation changes (Fig. 2g–i and Extended Data Fig. 3d).

Because cyclin D1–Cdk4 can phosphorylate other regulatory components of gluconeogenic pathway[20] (Extended Data Fig. 3e), we examined whether cyclin D1–Cdk4 kinase modulates glucose production through PGC-1α and GCN5. As expected, the induction of gluconeogenic genes by Cdk4 inhibition was completely blunted when PGC-1α was stably knocked down in liver cells (Extended Data Fig. 3f). Also, *Cdk4* knockdown did not increase glucose production and gluconeogenic gene expression in GCN5 depleted hepatocytes (Fig. 2j and Extended Data Fig. 3g). GCN5 AA had a marginal ability to suppress hepatic gluconeogenesis compared with GCN5 wild type, and showed no significant changes when combined with Cdk4 inhibition (Fig. 2k and Extended Data Fig. 3h). Together, these results strongly suggest that the effects of cyclin D1–Cdk4 on gluconeogenesis are mediated by the GCN5-PGC-1α complex.

We examined whether liver gluconeogenesis was altered when cyclin D1–Cdk4 kinase activity was manipulated in whole animals. When PD 0332991 was administered to re-fed mice, it increased *Pck1* expression and glycaemia without changing circulating insulin levels (Fig. 2l, m and Extended Data Fig. 3i, j). In contrast, hepatic cyclin D1 T286A expression significantly repressed fasting gluconeogenic genes, glycaemia and hepatic capacity to produce glucose as assessed by a pyruvate tolerance test (Fig. 2n–p and Extended Data Fig. 3k). We confirmed that PD 03322991 or cyclin D1 T286A adenoviral administration produced those physiological changes without causing liver toxicity (Extended Data Fig. 4a, b). Collectively, these data indicate that changes in hepatic cyclin D1–Cdk4 activity are sufficient to control hepatic gluconeogenesis and whole-body glucose homeostasis.

Next, we investigated whether cyclin D1–Cdk4 complex is regulated under nutritional and hormonal changes. In spite of parenchymal hepatocytes being post-mitotic, hepatic protein and messenger RNA (mRNA) expression of cyclin D1 were significantly increased upon 4 h re-feeding, which was not a strain-specific phenomenon (Fig. 3a, b and Extended Data Fig. 5a, b). This induction of cyclin D1 corresponded with elevated cyclin D1–Cdk4 activity, as observed by increases of Rb, GCN5 phosphorylation and elevated kinase activity of immunoprecipitated Cdk4 upon re-feeding (Fig. 3b, c and Extended Data Fig. 5c). Interestingly, cyclin D1 expression was regulated upon re-feeding only in liver, and Cdk4 inhibitor administration altered PGC-1α target genes only in liver and white adipose tissue (Extended Data Fig. 5d, e). Although Cdk4 regulates glucose metabolism in other tissues than liver, it is unknown whether this regulation is dependent on PGC-1α[21].

Cyclin D1–Cdk4 activity increased upon re-feeding was uncoupled from cell cycle progression. Known cell division markers did not change upon re-feeding (Extended Data Fig. 5f). Consistently, we found no difference in hepatocyte ploidy profile, Ki-67 expression levels and 5-bromodeoxyuridine (BrdU) incorporation between the livers of fasted and re-fed mice (Fig. 3d, e and Extended Data Fig. 5g). Alteration of cyclin D1–Cdk4 activity in liver by hepatic overexpression of cyclin D1 T286A or by a pharmacological inhibition caused no changes in cell cycle progression during fasting and re-feeding, as analysed by hepatic ploidy and Ki-67 expression (Extended Data Fig. 5h–j).

GSK-3β, active during fasting and inactive during re-feeding owing to its phosphorylation by insulin-AKT signalling, negatively regulates cyclin D1 through phosphorylation of T286, causing nuclear exclusion of cyclin D1 and proteasomal degradation[18,22]. We considered that insulin stimulation and subsequent inactivation of GSK-3β allow cyclin D1 to form an active complex with Cdk4, promoting PGC-1α acetylation. Insulin or two GSK-3β inhibitors increased nuclear cyclin D1 protein when tested in an overexpressed or endogenous manner (Fig. 3f and Extended Data Fig. 5k). This increase correlated with elevated PGC-1α acetylation and a significant reduction of gluconeogenic genes (Fig. 3g and Extended Data Fig. 5l). In accordance, insulin increased Cdk4-mediated GCN5 phosphorylation (Fig. 3h). Interestingly, we found that amino acids, but not insulin, increased cyclin D1 mRNA expression in primary hepatocytes (Extended Data Fig. 5m–o). To test if amino acids could be dietary components promoting cyclin D1 mRNA in liver, mice were fed with empty calorie, glucose only or glucose and amino-acid diets for 4 h. A significant cyclin D1 mRNA induction was observed only

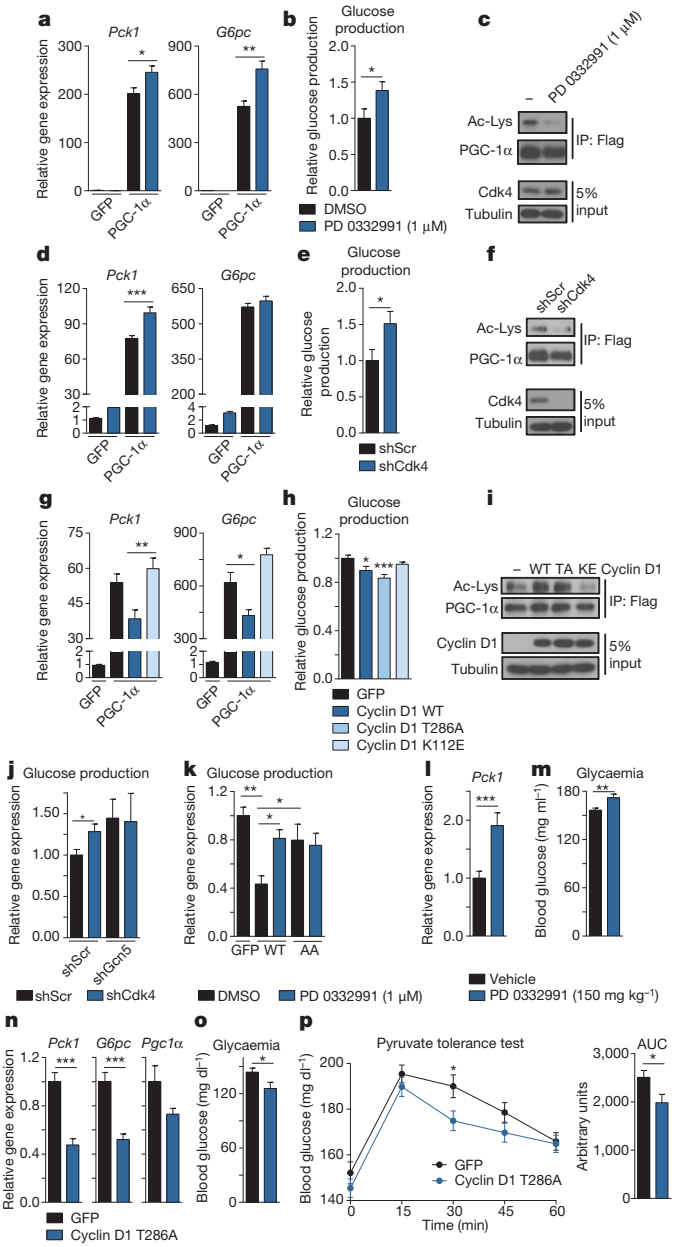

Figure 2 | Cyclin D1–Cdk4 regulates gluconeogenesis in primary hepatocytes and whole animals. **a**, **b**, PD 0332991 increases gluconeogenic gene expression and glucose production (**a**: one-way analysis of variance (ANOVA) with Tukey post-test, $n = 3$, **b**: two-tailed unpaired *t*-test, $n = 8$). **c**, PGC-1α acetylation is decreased by PD 0332991 treatment. **d**, **e**, *Cdk4* knockdown increases gluconeogenic gene expression and glucose production (**d**: one-way ANOVA with Tukey post-test, $n = 6$, **e**: two-tailed unpaired *t*-test, $n = 6$). **f**, PGC-1α acetylation is decreased upon Cdk4 deletion. **g**, **h**, Cyclin D1 wild-type decreases gluconeogenic gene expression, and cyclin D1 wild-type and cyclin D1 T286A, but not cyclin D1 K112E, repress glucose production (**g**: one-way ANOVA with Tukey post-test, $n = 3$/green fluorescent protein (GFP), PGC-1α, $n = 6$/cyclin D1 WT and KE, **h**: one-way ANOVA with Dunnett post-test, $n = 8$). **i**, Overexpression of cyclin D1 wild-type (WT) and T286A (TA), but not cyclin D1 K112E (KE), induces PGC-1α acetylation. **j**, *Gcn5* knockdown blunts the increase of glucose production by *Cdk4* knockdown (two-tailed unpaired *t*-test, $n = 8$). **k**, PD 0332991 increases glucose production with GCN5 wild type (WT), but not with GCN5 T272A/S372A (AA) (one-way ANOVA with Newman–Keuls post-test, $n = 8$). **l**, **m**, PD 0332991 administration increases *Pck1* gene expression and glycaemia in mice (two-tailed unpaired *t*-test, $n = 18$/vehicle, $n = 17$/PD 0332991). **n**, **o**, Gluconeogenic gene expression and glycaemia are reduced by cyclin D1 T286A overexpression in liver (two-tailed unpaired *t*-test, $n = 10$/GFP, $n = 9$/D1 T286A). **p**, Cyclin D1 T286A overexpression in liver decreases hepatic glucose production capacity assessed by pyruvate tolerance test (two-tailed unpaired *t*-test, $n = 20$/GFP, $n = 24$/D1 T286A; AUC, area under curve). All cells were infected with PGC-1α adenovirus for glucose production assays. Statistical significance is represented by asterisks corresponding to $^*P < 0.05$, $^{**}P < 0.01$ and $^{***}P < 0.001$. Data are shown as mean ± s.e.m.

when amino acids were added to the diet (Fig. 3i). These results indicate that amino acids contribute to the fed response along with insulin signalling to enhance cyclin D1 levels during re-feeding.

To test if cyclin D1–Cdk4 complex constitutes an important axis of the nutrient and insulin signalling to regulate glucose metabolism, we generated liver-specific cyclin D1 knockout ('D1 LKO') mice by crossing mice expressing a floxed cyclin D1 allele[23] with albumin-Cre-expressing mice[24]. Cyclin D1 deletion in liver did not interfere with liver development and caused no compensatory increases on other cyclins (Extended Data Fig. 5p, q). D1 LKO mice had similar gluconeogenic gene expression and glycaemia during fasting compared with wild-type mice, consistent with Cdk4 inactivation due to the absence of cyclin D1 (Fig. 3j, k). However, in the re-fed state, D1 LKO mice showed a significant increase in gluconeogenic genes and glycaemia compared with wild-type mice whereas induction of Rb phosphorylation and PGC-1α acetylation upon re-feeding were lacking (Fig. 3l, m and Extended Data Fig. 5r, s). Cdk4 inhibitor failed to increase gluconeogenic genes and glycaemia further in D1 LKO mice, suggesting cyclin D1 in liver mediates metabolic effects caused by Cdk4 inhibition (Extended Data Fig. 5t, u). Primary hepatocytes isolated from D1 LKO mice had increased gluconeogenic gene expression and higher glucose production than wild-type hepatocytes (Extended Data Fig. 5v, w). Consistent with elevated re-feeding blood glucose levels, D1 LKO mice showed moderate, yet significant, insulin and glucose intolerance, further indicating that cyclin D1–Cdk4 mediates, at least in part, insulin action in liver (Fig. 3n, o). When taken in aggregate, our findings indicate that insulin suppresses hepatic gluconeogenesis during re-feeding, in part by activating cyclin D1–Cdk4 complex to suppress PGC-1α activity.

Lastly, we investigated whether cyclin D1–Cdk4 activity was altered in diabetic mice. In the livers of fasted *Lepr*$^{db/db}$ mice, basal phosphorylations of AKT and its downstream targets were elevated, consistent with the hyperinsulinaemia of *db/db* mice (Fig. 4a). Accordingly, *db/db* mice had elevated fasted levels of cyclin D1 and phosphorylation of Rb, comparable to re-fed *db*/+ mice. In *db/db* mice, gluconeogenic genes and insulin signalling were refractory to fasting/re-feeding transitions, indicating an uncoupling of insulin signalling and its repressive effects on gluconeogenic programming (Fig. 4a and Extended Data Fig. 6a). We observed similar chronic elevations of cyclin D1 and insulin signalling impairment in mice fed a high-fat diet (Extended Data Fig. 6b). In accordance with chronic elevation of cyclin D1 in diabetic mice, phosphorylation of GCN5 remained higher, refractory to fasting/re-feeding transitions in diabetic compared with control mice (Extended Data Fig. 6c, d). These results suggest that in insulin-resistant mice compensatory hyperinsulinaemia maintains a chronically active cyclin D1–Cdk4 complex that is not sufficient to counteract increased gluconeogenesis. Hyperinsulinaemia might explain other studies showing different activities of insulin signalling in fasted diabetic animals[25,26].

We examined whether hyperactivation of cyclin D1–Cdk4 complex in *db/db* mice could alleviate hyperglycaemia. Hepatic overexpression of cyclin D1 T286A in *db/db* mice reduced gluconeogenic genes and glycaemia to *db*/+ mouse levels, whereas cyclin D1 K112E caused only minor suppressions of those parameters (Fig. 4b, c and Extended Data Fig. 6e). A similar pattern was observed in mice fed a high-fat diet (Extended Data Fig. 6f–h). We confirmed that cyclin D1 T286A overexpression in *db/db* mice indeed repressed hepatic glucose production by using hyperinsulinemic–euglycemic clamp experiments (Fig. 4d–h).

Our studies support a regulatory model in which insulin facilitates the formation of an active cyclin D1–Cdk4 complex that subsequently suppresses gluconeogenesis, in part by decreasing PGC-1α activity through

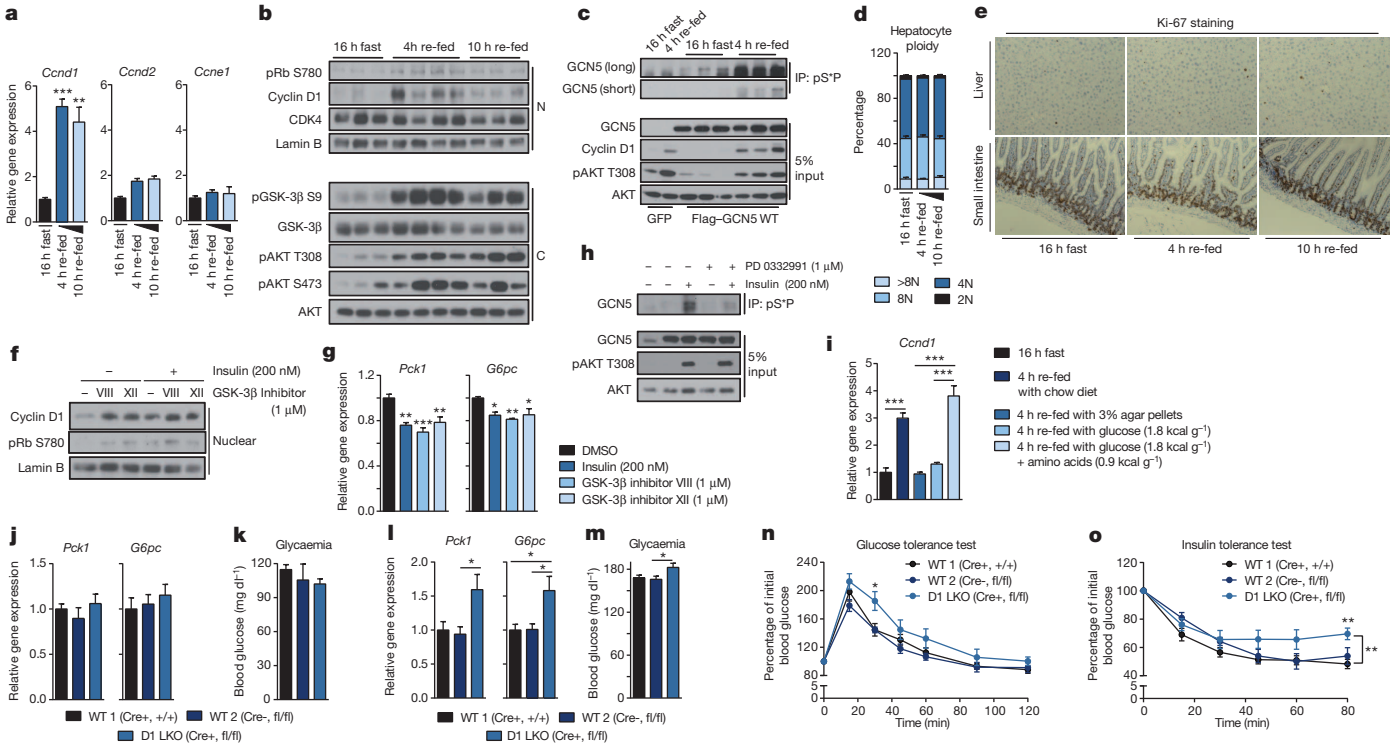

Figure 3 | Cyclin D1–Cdk4 is regulated by insulin/GSK-3β, and hepatic cyclin D1 deletion causes increased gluconeogenesis and glycaemia upon re-feeding. **a**, Cyclin D1 gene expression is increased during re-feeding (one-way ANOVA with Tukey post-test, $n = 3$/fast and10 h re-fed, $n = 4$/4 h re-fed). **b**, Cyclin D1 protein and Rb phosphorylation are induced upon re-feeding (N, nuclear, and C, cytoplasmic, liver extracts). **c**, Phosphorylation of GCN5 is increased upon re-feeding. GCN5 was immunoprecipitated using anti-phosphoS*P (pS*P) antibody from livers infected with GFP or GCN5 adenovirus. **d**, Hepatocyte ploidy does not change upon fasting and re-feeding ($n = 5$). **e**, Ki-67 staining in liver shows no differences upon fasting and re-feeding. Small intestine was used as a positive control. **f**, Nuclear cyclin D1 protein level is increased upon insulin and GSK-3β inhibitor treatment in primary hepatocytes. All cells were infected with cyclin D1 wild-type adenovirus. **g**, Insulin and GSK-3β inhibitors suppress gluconeogenic gene expression. All cells were infected with PGC-1α adenovirus (one-way ANOVA with Tukey post-test, $n = 6$). **h**, Phosphorylation of GCN5 is induced by insulin and blunted by PD 0332991 treatment. GCN5 was overexpressed whereas GFP was used as a negative control. **i**, Cyclin D1 is transcriptionally induced by dietary intake of amino acids. Mice were fasted overnight or re-fed 4 h with chow diet, empty calorie, glucose or glucose and amino-acid diet (one-way ANOVA with Tukey post-test, $n = 5$). **j**, **k**, Liver-specific cyclin D1 LKO mice show no differences on gluconeogenic gene expression and glycaemia during fasting. **l**, **m**, D1 LKO mice show increased gluconeogenic gene expression and glycaemia upon 4 h re-feeding (one-way ANOVA with Tukey post-test, combined four cohorts of $n = 3$/fasting, $n = 5$/re-feeding). **n**, D1 LKO mice show mild glucose intolerance (two-way ANOVA, multiple comparison, $n = 11$/WT1, $n = 7$/WT2, $n = 10$/D1 LKO). **o**, D1 LKO mice show mild insulin intolerance (two-way ANOVA, significant interaction, multiple comparison, $n = 10$/WT1, $n = 7$/WT2, $n = 9$/D1 LKO). Statistical significance is represented by asterisks corresponding to $^*P < 0.05$, $^{**}P < 0.01$, $^{***}P < 0.001$. Data are shown as mean ± s.e.m.

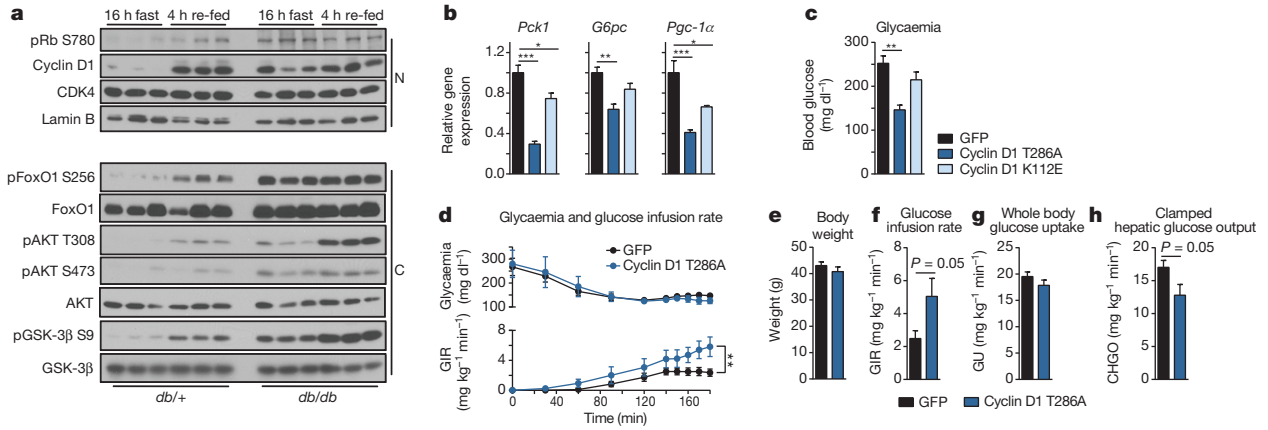

Figure 4 | In diabetic hyperinsulinemic mice, cyclin D1–Cdk4 is dysregulated and hyperactivation of cyclin D1–Cdk4 attenuates the diabetic phenotype. **a**, Cyclin D1 is chronically elevated in livers of *db/db* mice (N, nuclear, and C, cytoplasmic, liver extracts). **b**, **c**, Cyclin D1 T286A, but not cyclin D1 K112E, overexpression in liver represses gluconeogenic genes and glycaemia in *db/db* mice (one-way ANOVA, Tukey post-test, $n = 6$/GFP, D1 K112E, $n = 5$/D1 T286A). **d**–**h**, In *db/db* mice, cyclin D1 T286A overexpression in liver suppresses hepatic glucose production tested by hyperinsulinemic–euglycemic clamp. **d**, Plasma glycaemia and glucose infusion rate (GIR) (two-way ANOVA, significant interaction, $n = 7$). **e**, Body weights. **f**, Clamped glucose infusion rate. **g**, Whole-body glucose uptake (GU). **h**, Clamped hepatic glucose output (CHGO) (average of last 40 min values for **f**, **g**, two-tailed unpaired *t*-test for **d**–**h**, $n = 7$). Statistical significance is represented by asterisks corresponding to $^*P < 0.05$, $^{**}P < 0.01$, $^{***}P < 0.001$. Data are shown as mean ± s.e.m.

GCN5-mediated acetylation (Extended Data Fig. 6i). Under type 2 diabetic conditions, cyclin D1 protein levels are dysregulated owing to hyperinsulinaemia and insulin resistance, which contributes to its inability to repress gluconeogenesis fully during the fed state. In addition, cyclin D1 is also controlled at the transcriptional level by dietary intake of amino acids, further contributing to insulin's action, although the mechanisms are currently unknown. Despite the functional activation of cyclin D1–Cdk4 during re-feeding, hepatocytes undergo no cell cycle progression. Interestingly, genome-wide association studies have showed that mutations of CDKN2A, a Cdk4 inhibitor, are significantly correlated with a high risk of type 2 diabetes[27]. Combined with the role of cyclin D1–Cdk4 in β-islet pancreatic cell proliferation and the involvement of its target, E2F1, in oxidative metabolism[28,29], induction of gluconeogenesis in liver could predict the tendency of hyperglycaemia in cancer patients treated with Cdk4 inhibitors[30]. Future studies will address the metabolic functions of cell cycle components in different tissues and their use as therapeutic targets in metabolic diseases.

METHODS SUMMARY

The chemical screen was performed with a U-2OS cell line as described in Extended Data Fig. 1a. Immunoprecipitated GCN5 from cells infected with GCN5 adenoviruses was used for *in vitro* acetyltransferase activity assay. Glutathione *S*-transferase (GST)–cyclin D1–Cdk4, GST–Rb and 6 × His-GCN5 recombinant proteins were purchased whereas others were generated in the laboratory. Glucose levels in culture medium were measured with primary hepatocytes overexpressing PGC-1α. All animal studies were performed with 8- to 10-week-old male C57BL/6 mice unless indicated otherwise. PD 0332991 (150 mg kg^{-1}, pH 4) was administered by oral gavage. Adenoviruses were delivered by tail-vein injection with dosages of 1.5×10^9 to 2.0×10^9 infectious particles per animal. Pyruvate tolerance test was performed by intraperitoneal injection of pyruvate (2 g kg^{-1}) to overnight fasted mice whereas glucose tolerance (1 g kg^{-1}) and insulin tolerance tests (0.75 U kg^{-1}, diluted in PBS) were performed with mice fasted for 6 h. Diets containing empty calorie, glucose or glucose and amino acids were formulated in the laboratory. High-fat diet (60 kcal%) was administered to animals for 3 months before experiments. Detailed experimental procedures can be found in Methods.

Online Content Any additional Methods, Extended Data display items and Source Data are available in the online version of the paper; references unique to these sections appear only in the online paper.

Received 11 February 2013; accepted 20 March 2014.
Published online 25 May 2014.

1. Nakae, J., Park, B. C. & Accili, D. Insulin stimulates phosphorylation of the forkhead transcription factor FKHR on serine 253 through a wortmannin-sensitive pathway. *J. Biol. Chem.* **274,** 15982–15985 (1999).
2. Cho, H. *et al.* Insulin resistance and a diabetes mellitus-like syndrome in mice lacking the protein kinase Akt2 (PKBβ). *Science* **292,** 1728–1731 (2001).
3. Dentin, R. *et al.* Insulin modulates gluconeogenesis by inhibition of the coactivator TORC2. *Nature* **449,** 366–369 (2007).
4. Matsumoto, M., Pocai, A., Rossetti, L., Depinho, R. A. & Accili, D. Impaired regulation of hepatic glucose production in mice lacking the forkhead transcription factor Foxo1 in liver. *Cell Metab.* **6,** 208–216 (2007).
5. Puigserver, P. *et al.* Insulin-regulated hepatic gluconeogenesis through FOXO1-PGC-1α interaction. *Nature* **423,** 550–555 (2003).
6. Li, X., Monks, B., Ge, Q. & Birnbaum, M. J. Akt/PKB regulates hepatic metabolism by directly inhibiting PGC-1α transcription coactivator. *Nature* **447,** 1012–1016 (2007).
7. Estall, J. L. *et al.* Sensitivity of lipid metabolism and insulin signaling to genetic alterations in hepatic peroxisome proliferator-activated receptor-γ coactivator-1α expression. *Diabetes* **58,** 1499–1508 (2009).
8. Rodgers, J. T. *et al.* Nutrient control of glucose homeostasis through a complex of PGC-1α and SIRT1. *Nature* **434,** 113–118 (2005).
9. Lerin, C. *et al.* GCN5 acetyltransferase complex controls glucose metabolism through transcriptional repression of PGC-1α. *Cell Metab.* **3,** 429–438 (2006).
10. McKeehan, W. L., Adams, P. S. & Rosser, M. P. Direct mitogenic effects of insulin, epidermal growth factor, glucocorticoid, cholera toxin, unknown pituitary factors and possibly prolactin, but not androgen, on normal rat prostate epithelial cells in serum-free, primary cell culture. *Cancer Res.* **44,** 1998–2010 (1984).
11. Ish-Shalom, D. *et al.* Mitogenic properties of insulin and insulin analogues mediated by the insulin receptor. *Diabetologia* **40** (suppl 2), S25–S31 (1997).
12. Soni, R. *et al.* Inhibition of cyclin-dependent kinase 4 (Cdk4) by fascaplysin, a marine natural product. *Biochem. Biophys. Res. Commun.* **275,** 877–884 (2000).
13. Matsushime, H. *et al.* Identification and properties of an atypical catalytic subunit (p34PSK-J3/cdk4) for mammalian D type G1 cyclins. *Cell* **71,** 323–334 (1992).
14. Kato, J., Matsushime, H., Hiebert, S. W., Ewen, M. E. & Sherr, C. J. Direct binding of cyclin D to the retinoblastoma gene product (pRb) and pRb phosphorylation by the cyclin D-dependent kinase CDK4. *Genes Dev.* **7,** 331–342 (1993).
15. Fry, D. W. *et al.* Specific inhibition of cyclin-dependent kinase 4/6 by PD 0332991 and associated antitumor activity in human tumor xenografts. *Mol. Cancer Ther.* **3,** 1427–1438 (2004).
16. Boyer, L. A. *et al.* Essential role for the SANT domain in the functioning of multiple chromatin remodeling enzymes. *Mol. Cell* **10,** 935–942 (2002).
17. Rodgers, J. T. & Puigserver, P. Fasting-dependent glucose and lipid metabolic response through hepatic sirtuin 1. *Proc. Natl Acad. Sci. USA* **104,** 12861–12866 (2007).
18. Diehl, J. A., Zindy, F. & Sherr, C. J. Inhibition of cyclin D1 phosphorylation on threonine-286 prevents its rapid degradation via the ubiquitin-proteasome pathway. *Genes Dev.* **11,** 957–972 (1997).
19. Hinds, P. W., Dowdy, S. F., Eaton, E. N., Arnold, A. & Weinberg, R. A. Function of a human cyclin gene as an oncogene. *Proc. Natl Acad. Sci. USA* **91,** 709–713 (1994).
20. Anders, L. *et al.* A systematic screen for CDK4/6 substrates links FOXM1 phosphorylation to senescence suppression in cancer cells. *Cancer Cell* **20,** 620–634 (2011).
21. Abella, A. *et al.* Cdk4 promotes adipogenesis through PPARgamma activation. *Cell Metab.* **2,** 239–249 (2005).
22. Diehl, J. A., Cheng, M., Roussel, M. F. & Sherr, C. J. Glycogen synthase kinase-3beta regulates cyclin D1 proteolysis and subcellular localization. *Genes Dev.* **12,** 3499–3511 (1998).
23. Choi, Y. J. *et al.* The requirement for cyclin D function in tumor maintenance. *Cancer Cell* **22,** 438–451 (2012).
24. Pinkert, C. A., Ornitz, D. M., Brinster, R. L. & Palmiter, R. D. An albumin enhancer located 10 kb upstream functions along with its promoter to direct efficient, liver-specific expression in transgenic mice. *Genes Dev.* **1,** 268–276 (1987).
25. Macotela, Y. *et al.* Dietary leucine–an environmental modifier of insulin resistance acting on multiple levels of metabolism. *PLoS ONE* **6,** e21187 (2011).
26. Wang, Y. *et al.* Inositol-1,4,5-trisphosphate receptor regulates hepatic gluconeogenesis in fasting and diabetes. *Nature* **485,** 128–132 (2012).
27. Zeggini, E. *et al.* Replication of genome-wide association signals in UK samples reveals risk loci for type 2 diabetes. *Science* **316,** 1336–1341 (2007).
28. Rane, S. G. *et al.* Loss of Cdk4 expression causes insulin-deficient diabetes and Cdk4 activation results in β-islet cell hyperplasia. *Nature Genet.* **22,** 44–52 (1999).
29. Blanchet, E. *et al.* E2F transcription factor-1 regulates oxidative metabolism. *Nature Cell Biol.* **13,** 1146–1152 (2011).
30. Schwartz, G. K. *et al.* Phase I study of PD 0332991, a cyclin-dependent kinase inhibitor, administered in 3-week cycles (Schedule 2/1). *Br. J. Cancer* **104,** 1862–1868 (2011).

Acknowledgements We thank all the members of the Puigserver laboratory for discussions and suggestions about this project. We also appreciate the consultations with and efforts by M. Jedrychowski and S. Gygi for proteomic analysis. Y.L. was supported in part by a 21st Century Leaders scholarship from Ewha Womans University. J.E.D. was supported in part by a National Research Service Award Kirschstein Fellowship from the National Institutes of Health (NIH). The participating researchers were supported with funds from the Dana-Farber Cancer Institute and with grants from the American Diabetes Association, Department of Defense, NIH/National Institute of Diabetes and Digestive and Kidney Diseases (RO1069966 and R24DK080261-06), NIH (RO3 MH092174) awarded to P.P., NIH (RO1 CA108420) awarded to P.S. and NIH (DK059635) awarded to Yale's Mouse Metabolic Phenotyping Center/G.I.S.

Author Contributions P.P. and Y.L. conceived the project. Y.L. designed and performed most of the experiments aided by discussions with P.P. J.E.D. also contributed to the design and discussions of the manuscript. Additional advice in the design and execution of the experiments was provided by F.V. and J.-H.L. H.C. assisted with mice experiments. Y.J.C. and P.S. provided D1 fl/fl mice and helped with BrdU incorporation and Ki-67 staining experiments. M.J., J.P.C., H.-B.R., X.Y. and G.I.S. performed hyperinsulinemic–euglycemic clamp experiments, and analysed, interpreted and discussed the data. N.T. assisted with performance and analysis of chemical screening. Y.L. and P.P. wrote the manuscript.

Author Information Reprints and permissions information is available at www.nature.com/reprints. The authors declare no competing financial interests. Readers are welcome to comment on the online version of the paper. Correspondence and requests for materials should be addressed to P.P. (pere_puigserver@dfci.harvard.edu).

METHODS

Animal experiments. Eight- to 10-week-old male BALB/c mice and 8- to 10-week-old male C57BL/6 mice were purchased from Taconic Farms. Ten-week-old male BKS.Cg-Dock7^{m} +/+ *Lepr^{db}*/J heterozygous (*db*/+) and homozygous (*db*/*db*) mice were from Jackson Laboratory. After a delivery of mice to the animal facility, a 1-week acclimation period was given before experiments. No randomization and blind techniques were applied in this study. Liver-specific cyclin D1 LKO mice were generated by crossing mice expressing a floxed cyclin D1 allele (mixed background between 129/SvJ and C57BL/6 and backcrossed to C57BL/6 for five times)[23] with albumin-Cre-expressing mice[24]. High fat diet (60 kcal%) (D12492i) and its control diet (D12450J) were administered to animals for 3 months before experiments.

PD 0332991 was dissolved in 20 mM sodium lactate solution made at pH 4.0. The compound (150 mg kg^{-1}) or buffer solution was given to each mouse once per day by oral gavage. After two consecutive administrations, all mice were killed upon 4 h re-feeding followed by overnight fasting, except the administration was reduced to once in the experiments with D1 LKO mice. To overexpress cyclin D1 T286A or K112E in liver, adenoviruses were injected through the tail vein and GFP adenovirus was used as a negative control (all constructs with 1.5×10^9 infectious particles per lean mouse and 2.0×10^9 per obese mouse). All mice were killed after 4 days of injection followed by overnight fasting unless indicated otherwise (the fasting started 1 h after the dark-cycle initiated in the facility). Before being killed, all mice were tail bled to measure glycaemia using Precision Xtra from Abbott Diabetes Care. Upon collection, livers were removed and snap frozen in liquid nitrogen until processed.

For BrdU incorporation, 100 μg g^{-1} body weight was given intraperitoneally 16 h before collection. For RNA extraction from pancreas, we followed the modified protocol previously reported[31] and the quality of RNA samples was verified by 28S/18S presence using 1% agarose gel electrophoresis. For diet experiments, 3% agar was autoclaved and mixed with glucose (1.8 kcal g^{-1}), amino acids (0.9 kcal g^{-1}) or both. Each amino acid was weighed and mixed as LabDiet (5001) formula indicates. For the pyruvate tolerance test, pyruvate (2 g kg^{-1}, dissolved in PBS) was injected intraperitoneally to overnight-fasted mice, 4 days after adenoviral injections. For the glucose tolerance and insulin tolerance tests, mice were fasted for 6 h before injection and glucose (1 g kg^{-1} dissolved in PBS) and insulin (0.75 U kg^{-1} diluted in PBS) were delivered by intraperitoneal injection. Glycaemia was monitored by tail-bleeding every 15–20 min; if hypoglycaemia caused by insulin injection was observed, 1 g kg^{-1} glucose was injected and the mice was exempted from experiment. All animal experiments were designed and conducted by following the Dana-Farber's Institutional Animal Care and Use Committee.

Insulin and serum biochemistry measurement. Upon being killed, serum samples were gathered from blood collected by cardiac puncture. Insulin was measured with Ultra Sensitive Mouse Insulin ELISA Kit (Crystal Chem, 90080). All kits used to measure serum biochemistry including alanine transaminase (EALT-100), aspartate transaminase (EASTR-100), lactate dehydrogenase (DLDH-100), creatine kinase (ECPK-100) and total bilirubin (DIBR-100) were purchased from Bioassay Systems.

High-throughput chemical screening. U-2OS human osteosarcoma cells were infected with Flag-tagged PGC-1α and GCN5 expressing adenovirus and were split to 384-well plates. The chemical compounds were added to the cells and incubated overnight. Cells were collected and lysates were transferred to enzyme-linked immunosorbent assay (ELISA) plates (Nunc, 460372) coated with M2 FLAG-antibody (Sigma, F1804) to immunoprecipitate PGC-1α. The plates were washed with PBST buffer, and acetylated-lysine antibody (Cell Signaling, 9441) was added to detect the acetylation level of PGC-1α. After primary antibody incubation, horseradish peroxidase (HRP)-IgG-Rabbit antibody (Jackson Immuno Research, 711035152) was added as a secondary antibody. A plate reader recorded the signal after incubating the plates with HRP-reacting ELISA substrate (Thermo Scientific, 37069) to generate chemiluminescence at 425 nm. Further details for the screening conditions are available upon request.

Adenoviruses, constructs and recombinant information. All adenoviruses were generated by using the pAdTrack/pAdEasy system and amplified in HEK293A cells. Adenoviruses were purified by caesium chloride gradient centrifugation and dialysed in Tris-HCl buffer made at pH 8 before use. Flag–HA-PGC-1α (mouse) and Flag–GCN5 (mouse) adenoviruses were made as previously described[8,9]. Flag–cyclin D1 wild-type and K112E (mouse) adenoviruses were generated by subcloning from reported constructs given by P. Sicinski. Flag–cyclin D1 T286A (human) was subcloned from a construct obtained from Addgene deposited by B. Zetter. Adenovirus with short-hairpin RNA was driven by a U6 promoter and subcloned from a pLKO.1 vector. pLKO.1 vector with shRNA against mouse Cdk4 construct targeting 5′-CCTAGCTAGAATCTACAGCTA-3′ was obtained from the Dana-Farber RNAi Screening Facility. pLKO.1 vectors with shRNA containing scrambled sequence 5′-CAACAAGATGAAGAGCACCAA-3′ were used to generate a control virus.

The sequence of shGcn5 against GCN5 was previously used and described[9]. pLKO.1 vectors with various shRNAs against human Cdk4 were obtained from the Dana-Farber RNAi Screening Facility with the following sequences; shCdk4#1 5′-GACACTGAGAGGGCAATCTTT-3′, shCdk4#2 5′-GTGGAGTGTTGGCTGTATCTT-3′, shCdk4#3 5′-CATGCCAATTGCATCGTTCAC-3′, shCdk4#4 5′-GAGATTACTTTGCTGCCTTAA-3′, and shCdk4#5 5′-GTTCTTCTGCAGTCCACATAT-3′.

Cell lines and primary hepatocytes cultures. HEK293A, U-2OS, HepG2 cells were purchased from ATCC (CRL-1573, HTB-96 and HB-8065) and maintained in DMEM containing 10% FBS under 5% CO_2 condition. All transformed cells were tested negative for mycoplasma using a PCR mycoplasma detection kit (Takara Bio, 6601). All constructs were transfected using Polyfect (Qiagen, 301105) and cells were collected after 48 h or 72 h of transfection. Medium was changed every day as well as 3 h before collection. For U-2OS cells, 1 μM Cdk4 inhibitors were added 8 h before collection. Dimethylsulphoxide (DMSO) was used as a negative control treatment for all chemical treatments used in this study. Lentiviral shRNAs for shScr and Pgc1α were produced by transfecting HEK293A cells with pLKO.1 shScr and shPgc1α; the sequences of shRNAs have been reported previously[32]. Control and PGC-1α stably knocked down HepG2 cells were generated by infecting cells with lentiviral particles and selected with puromycin for a week.

Primary hepatocytes were isolated from 8- to 10-week-old male BALB/c mice by perfusion with liver digest medium (Invitrogen, 17703-034) followed by 70 μm mesh filtration. Percoll (Sigma, P7828) gradient centrifugation allowed primary hepatocytes isolation from other cell types and debris. On six-well plates, 4×10^5 cells per well were seeded in plating medium (DMEM with 10% FBS, 2 mM sodium pyruvate, 1% penicillin/streptomycin, 1 μM dexamethasone, and 100 nM insulin). After 3 h of seeding, the medium was changed and incubated overnight in maintenance medium (DMEM, 0.2% BSA, 2 mM sodium pyruvate, 1% penicillin/streptomycin, 0.1 μM dexamethasone, and 1 nM insulin). To infect cells with adenovirus, 3×10^6 to 8×10^6 infectious particles per well were added to cells for 4 h. Cells were collected within 48 h after infection and medium was changed everyday as well as 3 h before collection. Cdk4 inhibitors and GSK-3β inhibitors (1 μM) were added overnight whereas 200 nM insulin was added 1.5 h before collection. When necessary, the medium was changed to starvation medium (DMEM, 0.2% BSA, 2 mM sodium pyruvate, and 1% penicillin/streptomycin) for 3 h and cells were stimulated with 10 μM forskolin for an extra 1.5 h. When glucose production was measured, cells were incubated in starvation medium for 2 h followed by incubation for 3 h in glucose-free medium (phenol-red/glucose free DMEM, 0.2% BSA, 2 mM sodium pyruvate and 20 mM sodium lactate). The glucose level in the medium was measured by glucose assay kit from Bioassay Systems (EBGL-100) following the manufacturer's instructions. For amino-acid addition, primary hepatocytes were incubated overnight with amino-acid-free medium (Earl's balanced salt solution, 25 mM glucose, 2 mM sodium pyruvate, 1% penicillin/streptomycin, BME vitamin mix and 0.2% fatty-acid-free BSA). Cells were collected after incubation for 4 h with 4 mM HEPES-KOH pH 7.4 buffer, minimum essential medium (MEM) amino acids or non-essential amino acids.

Cell lysis, immunoprecipitation and western blot analysis. In the case of PGC-1α acetylation detection from PGC-1α overexpressed cells, cells were collected in RIPA buffer (containing protease inhibitor cocktail, 5 mM NaF, 5 mM glycerate-2-phosphate, 20 mM nicotinamide, 1 μM DTT and 1 μM trichostatin A). Flag–HA-PGC-1α was immunoprecipitated with Flag-beads (Sigma A2220). For endogenous PGC-1α immunoprecipitation, cells or pulverized tissues were incubated with buffer A to obtain nuclear pellets (buffer A: 10 mM HEPES-KOH pH 7.9, 10 mM KCl, 1.5 mM $MgCl_2$, 0.25% Igepal and reagents mentioned above). Once cytoplasmic fractions were removed, nuclear pellets were lysed in RIPA buffer without SDS. From the lysate, endogenous PGC-1α was immunoprecipitated by anti-PGC-1α antibody (Santa Cruz Biotechnology sc-13067) coupled with Dynabeads protein A (GE Lifescience 1001D). For endogenous co-immunoprecipitation experiments, proteins from nuclei were extracted in CHAPS based lysis buffer (10 mM HEPES-KOH pH 7.4, 150 mM NaCl, 0.5% Igepal, 0.3% CHAPS, 10% glycerol and reagents mentioned above). The lysate was pre-cleared with protein A (GE Lifescience 17-0780-01), and anti-Cdk4 antibody (Santa Cruz Biotechnology sc-260) was added to the immunoprecipitate. GCN5 pull-down with anti-phospho-S*P antibody was performed with whole-cell lysates extracted with RIPA buffer without SDS followed by protein A pre-clearing and incubation with anti-phospho-S*P antibody (Cell Signaling 2325). All immunoprecipitated samples were washed at least four times with lysis buffer. For all endogenous immunoprecipitation experiments, rabbit IgG antibody was used as a negative control.

The following antibodies were used for western blot analysis: anti-PGC-1α (sc-13067), anti-Cdk4 (sc-260) and anti-cyclin D1 (sc-450) from Santa Cruz Biotechnology; anti-acetylated-lysine (9441), anti-GCN5 (3305), anti-pSer780 Rb (3590 or 8180), anti-Rb (9313), anti-cyclin D1 (2978), anti-pThr308 AKT (2965), anti-pSer473 AKT (4060), anti-AKT (9272), anti-pSer9 GSK-3β (9323) and anti-GSK-3β (9315) from Cell Signaling; anti-Lamin B (ab16048) and anti-Rabbit IgG (ab37415) from Abcam; anti-tubulin (05-661) from Millipore; anti-Flag (A8592) and anti-βactin (A2228) from Sigma. Anti-PAF65-β antibody was given by Y. Nakatani[33].

***In vitro* Cdk4/cyclin D1 kinase assay.** GST–cyclin D1–Cdk4 complex (0142-0143-1) and GST–Rb (733–928 amino acids, 0040-0000-6) were purchased from ProQinase and 6xHis-GCN5 full length (ALX-201-280-C002) was from Enzo Life Science. Recombinant GST–GCN5 proteins (1–224 amino acids, 1–386 amino acids, 1–553 amino acids, 1–837 amino acids) were generated with pGEX–5X–2 vectors containing the corresponding sequences of mouse GCN5. pGEX–2X–GST–FoxO1 (1–300 amino acids) and FoxO1 (290–570 amino acids) were a gift from A. Banks. pGEX 4T-3 FoxO3A was purchased from Addgene deposited by M. Greenberg. GST–PGC-1α SR domain protein was generated in the laboratory[34]. For the comparison between GCN5 and Rb phosphorylation, 6 × His-GCN5 (200 ng), GST–Rb (150 ng) and GST–cyclin D1–Cdk4 (50 ng) were used in the assay. Kinase reactions were performed in a kinase buffer (50 mM HEPES-KOH buffered at pH 7.5, 10 mM $MgCl_2$) with 20 μM ATP, 1 mM DTT and 2.5 μCi of [γ-^{32}P]ATP from Perkin Elmer (BLU002A250UC). The reaction was incubated at 30 °C for 30 min and terminated by adding SDS sample buffer and boiling at 100 °C for 5 min. Recombinant proteins were analysed after SDS–polyacrylamide gel electrophoresis separation and silver-stained with a SilverQuest silver staining kit from Invitrogen (LC6070).

For *in vitro* kinase assay with immunoprecipitated cyclin D1–Cdk4 kinase from liver, lysates were extracted from pulverized livers by using Ipegal based buffer (20 mM HEPES-KOH pH 7.9, 125 mM NaCl, 1 mM EDTA, 1% Ipegal, protease inhibitor cocktail, 5 mM NaF, 5 mM glycerate-2-phosphate, 20 mM nicotinamide, 1 μM DTT and 1 μM trichostatin A). Cyclin D1–Cdk4 kinase was immunoprecipitated from 400 μg of lysates by anti-Cdk4 antibody and rabbit IgG antibody was used as a negative control. Kinase reactions were performed with 2.5 μg of recombinant Rb in a similar condition as described above except 5 mM NaF and 5 mM glycerate-2-phosphate were included in a kinase buffer.

***In vitro* GCN5 acetyltransferase activity assay.** Flag–GCN5 was immunoprecipitated with Flag-beads from nuclear lysates of U-2OS cells that were infected with GCN5 adenoviruses and treated with DMSO or 1 μM fascaplysin. Flag–GCN5 protein was eluted from the beads by rotating the lysates and beads with 3 × FLAG peptide (Sigma F4799) at 4 °C for 2 h. The eluates were further purified using Amicon centrifugal filters (Millipore UFC5030). Following the manufacturer's instructions, the enzymatic activity was measured using a fluorimetric acetyltransferase assay kit (Active Motif 56100). Kinetic constants were calculated with the Michaelis–Menten equation based on arbitrary fluorescence units generated during 15 min reaction.

Gene expression analysis. Total RNA was isolated with Trizol (Invitrogen, 15596-026). Two micrograms of RNA were used to generate complementary DNA (cDNA) with a High Capacity cDNA Reverse Transcription Kit (Applied Biosystmes, 4368813) following the manufacturer's protocol. For gene expression analysis, cDNA samples were mixed with Sybr Green qPCR mastermix (Applied Biosystem 4309155) and were analysed by a CFX384 Real-Time system from Bio-Rad. All primers and sequences are available upon request.

FACS analysis for hepatocytes ploidy profile. Primary hepatocytes were isolated as described above. The cells were suspended in PBS and 1×10^6 cells were added drop-by-drop to pre-chilled 75% ethanol for 30 min. Ethanol was aspirated and cells were washed and re-suspended in PBS with RNase A (Invitrogen, 12091-021) at a final concentration of 70 units per millilitre. Propidium iodide (BD Biosciences, 556463) was added at a final concentration of 5 μg ml^{-1} to the cells and incubated for 30 min with brief vortexing in between. The samples were protected from light until analysed with BD FACSCanto II.

BrdU and Ki-67 staining. Upon being killed, liver and small intestine were collected. Liver was washed in PBS briefly and the small intestine was flushed and washed with PBS. Tissues were fixed in 4% formaldehyde for 48 h and transferred to 70% ethanol before being paraffin-embedded and sectioned. Anti-BrdU antibody (B2531) was from Sigma. The antibody was run on an automated platform, Leica BOND-III. The retrieval step used Leica's ER1 solution for 30 min, and the primary antibody was incubated at 1:2,000 dilution for 30 min. A Bond Polymer Refine Detection kit was used, which included the secondary and DAB chromogen detection. The Ki-67 was also run on the BOND-III using the same detection kit. Anti-Ki-67 antibody (VP-RM04) was from Vector and was incubated at 1:250 dilution for 30 min. The retrieval solution used on the BOND-III was Leica's ER2 antigen retrieval solution and incubated for 20 min.

Hyperinsulinemic–euglycemic clamp studies. Hyperinsulinemic–euglycemic clamps were performed as previously reported with minor modifications[35]. Mice were operated to implant an indwelling catheter in the right jugular vein 7 days before study. Four days before study, mice were infected with GFP or cyclin D1 T286A adenovirus by tail-vein injection. After overnight fasting, mice were infused with a fixed amount of insulin (40 mU kg^{-1} min^{-1}) and a variable amount of 20% dextrose to maintain euglycaemia. 3-[^{3}H]glucose was included in the infusates to trace whole-body rates of glucose metabolism. Whole-body glucose uptake was determined under steady-state conditions during the final 40 min of the clamp when exogenous glucose infusion and endogenous glucose production were in equilibrium with whole-body disposal. Whole-body glucose disposal was calculated as the ratio of the 3-[^{3}H]glucose infusion rate and the specific activity of plasma glucose; hepatic glucose production represents the difference between the glucose infusion rate and whole-body uptake calculation.

Statistics. All statistics are described in figure legends. In general, for two experimental comparisons, a two-tailed unpaired Student's *t*-test was used. For multiple comparisons, one-way ANOVAs with Tukey, Newman–Keuls or Dunnett post-test were applied. For the glucose tolerance test, insulin tolerance test and hyperinsulinemic–euglycemic clamp, a two-way ANOVA with repeated comparison was applied. When cells were used for experiments, three replicates per treatment were chosen as an initial sample size. All *n* values defined in the legends refer to biological replicates unless otherwise indicated. All western blot analysis was repeated at least three times. In mice experiments requiring technical manipulations, at least seven mice were used per treatment based on our previous experiences. If technical failures such as tail-vein injection failure, inadequate intraperitoneal injection and oral gavage occurred before collection, those samples were excluded from the final analysis. Statistical significance is represented by asterisks corresponding to $*P < 0.05$, $**P < 0.01$, $***P < 0.001$.

31. Li, D. *et al.* A modified method using TRIzol reagent and liquid nitrogen produces high-quality RNA from rat pancreas. *Appl. Biochem. Biotechnol.* **158,** 253–261 (2009).
32. Vazquez, F. *et al.* PGC1α expression defines a subset of human melanoma tumors with increased mitochondrial capacity and resistance to oxidative stress. *Cancer Cell* **23,** 287–301 (2013).
33. Ogryzko, V. V. *et al.* Histone-like TAFs within the PCAF histone acetylase complex. *Cell* **94,** 35–44 (1998).
34. Rodgers, J. T., Haas, W., Gygi, S. P. & Puigserver, P. Cdc2-like kinase 2 is an insulin-regulated suppressor of hepatic gluconeogenesis. *Cell Metab.* **11,** 23–34 (2010).
35. Jurczak, M. J. *et al.* Dissociation of inositol-requiring enzyme (IRE1α)-mediated c-Jun N-terminal kinase activation from hepatic insulin resistance in conditional X-box-binding protein-1 (XBP1) knock-out mice. *J. Biol. Chem.* **287,** 2558–2567 (2012).

a

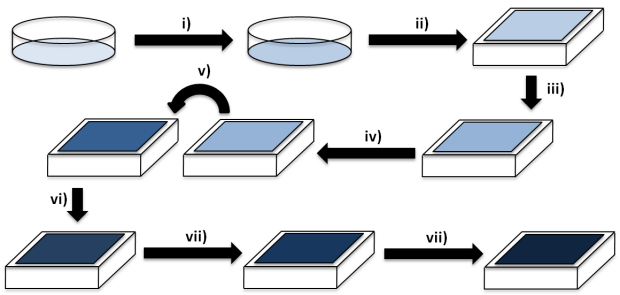

i) U-2OS cells are infected with PGC-1α and GCN5 adenoviruses
ii) Cells are split to 384 well plates and settled for 10 h
iii) Compounds are added and incubated with cells overnight
iv) Cells are lysed and the lysates are transferred to anti-Flag coated ELISA plates
v) Upon removal of the lysates, anti-Ac-Lys is added and incubated for 1 h at 37 °C
vi) After removal of primary antibody, anti-Rabbit-HRP is added and incubated for 30 min at 37°C
vii) Secondary antibody is washed off and ELISA substrates are added and plates are read

b

Compounds Inducing Hyperacetylation of PGC-1α

Compound Name	Known Function	Z Score
Scriptaid	Histone Deacetylase Inhibitor	5.190337
Calyculin A	Serine/Threonine Phosphatase Inhibitor	3.686409
NC*		3.382186
NC		3.145855

Compounds Inducing Deacetylation of PGC-1α

Compound Name	Known Function	Z Score
Fascaplysin	CDK4 Inhibitor	-3.99137
NC		-3.47384
NC		-3.29365
NC		-3.27336
NC		-3.17319
Homoharringtonine	Protein Translation Inhibitor	-3.14736
NC		-3.11901
NC		-3.08834
Emetine Dihydrochloride	Protein Synthesis Inhibitor	-3.06788
LY-83583	An Inhibitor of Soluble Guanylate Cyclase and of cGMP Production	-3.02671

*NC = Natural Compound

Extended Data Figure 1 | A cell-based high-throughput screen shows compounds regulating PGC-1α acetylation. **a**, Scheme of high-throughput chemical assay. **b**, Compounds with significant *z* scores either greater than 3.0 or less than −3.0 are listed. Inhibitors indicate the compounds that increased PGC-1α acetylation whereas activators indicate those that decreased PGC-1α acetylation.

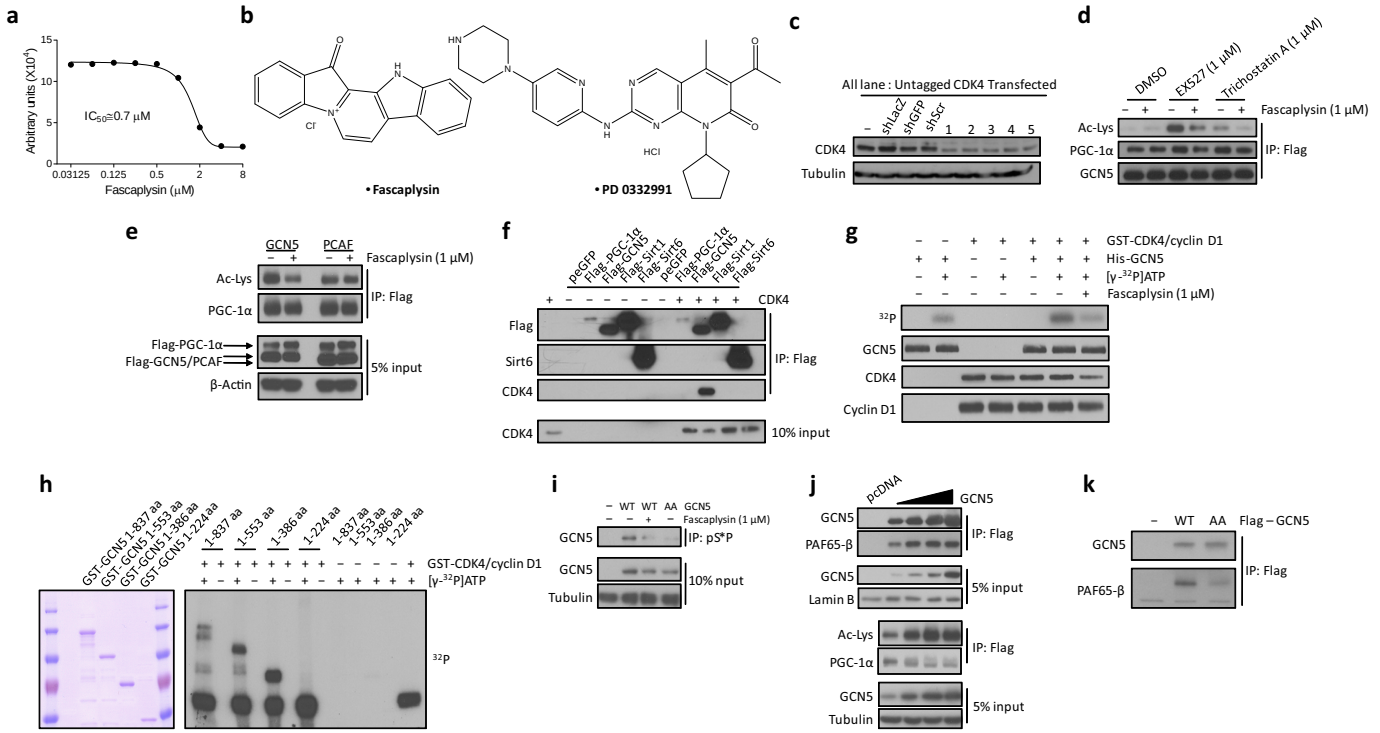

Extended Data Figure 2 | Cyclin D1–Cdk4 modulates PGC-1α acetylation through GCN5. **a**, Fascaplysin decreases PGC-1α acetylation in a dose-dependent manner. The dose-dependent response of PGC-1α acetylation treated with fascaplysin concentrations ranging from 31.25 nM to 8 μM was analysed by western blotting. The IC_{50} value was calculated using three independent measurements from the assay described in Extended Data Fig. 1a. **b**, Chemical structures of fascaplysin and PD 0332991. **c**, *Cdk4* is knocked down by various *Cdk4* shRNAs used in Fig. 1d. **d**, Fascaplysin decreases PGC-1α acetylation upon EX527 or trichostatin A treatments. Cells were treated for 8 h in the case of 1 μM fascaplysin and 4 h in the case of 1 μM EX527 or trichostatin A before collection. DMSO (-) was used as a control treatment. **e**, Fascpalysin has blunted effect on PCAF-mediated PGC-1α acetylation. **f**, Ectopically expressed Cdk4 and GCN5 interact. As a comparison, PGC-1α, Sirt1 and Sirt6 were used whereas GFP was overexpressed as a negative control. **g**, Phosphorylation of GCN5 by cyclin D1–Cdk4 complex is reduced by fascaplysin. DMSO or 1 μM fascaplysin were added to the kinase reaction. **h**, *In vitro* phosphorylation of GST–GCN5 recombinant proteins (1–224 amino acids, 1–386 amino acids, 1–553 amino acids, 1–837 amino acids) by cyclin D1–Cdk4 and the protein level of those fragments. **i**, GCN5 wild type (WT), treated with fascaplysin and GCN5 T272A/S372A (AA) mutant immunoprecipitated by anti-phospho-S*P (pS*P) antibody. **j**, Acetylation of PGC-1α closely follows the amount of PAF65-β bound to GCN5. Nuclear extracts of U-2OS overexpressing various amounts of GCN5 were used for western blot analysis to detect GCN5 and PAF65-β. Empty vector was transfected as a negative control. **k**, Interaction between GCN5 T272A/S372A (AA) and PAF65-β is reduced compared with GCN5 wild type (WT). U-2OS cells were used for western blot analysis experiments.

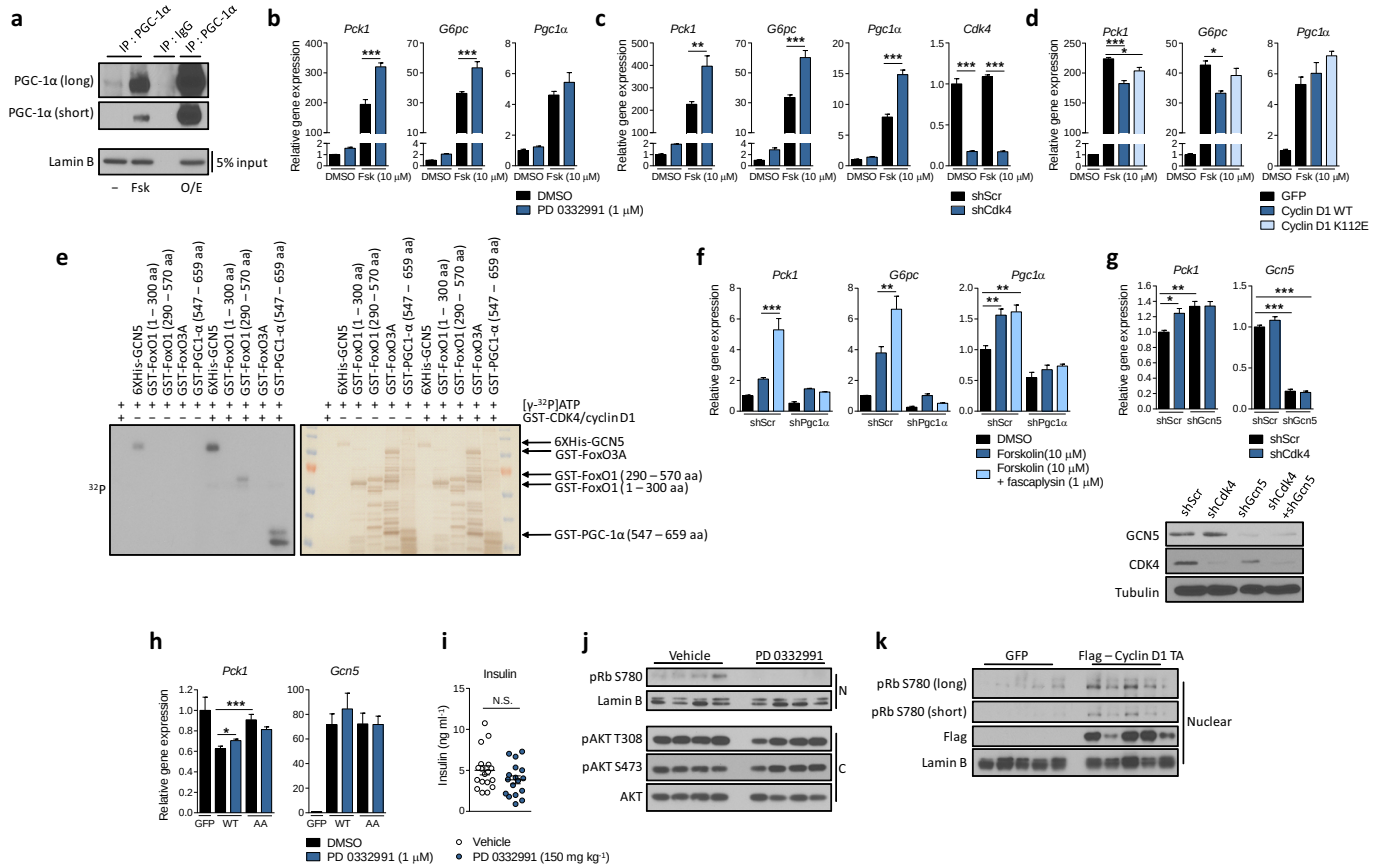

Extended Data Figure 3 | Cyclin D1–Cdk4 regulates gluconeogenesis in primary hepatocytes and in whole animals. **a**, Western blot analysis of endogenous, forskolin-induced (Fsk) or adenovirally overexpressed (O/E) PGC-1α. Nuclear extracts of primary hepatocytes were used to immunoprecipitate PGC-1α. Cells were infected with GFP or PGC-1α 48 h before collection. Forskolin (10 μM) was added for 2 h before collection. **b**, PD 0332991 increases forskolin-induced gluconeogenic gene expression. Primary hepatocytes were treated with 10 μM forskolin for 1.5 h after 3 h of starvation medium incubation while 1 μM PD 0332991 was added overnight (one-way ANOVA with Tukey post-test, $n = 3$). **c**, *Cdk4* knockdown increases forskolin-induced gluconeogenic gene expression (one-way ANOVA with Tukey post-test, $n = 3$). **d**, Cyclin D1 wild-type, but not cyclin D1 K112E mutant, suppresses forskolin-induced gluconeogenic gene expression (one-way ANOVA with Tukey post-test, $n = 3$). **e**, Phosphorylation of GCN5, FoxO1 amino (N) terminus, FoxO1 carboxy (C) terminus, FoxO3A and PGC-1α SR domain by cyclin D1–Cdk4. **f**, *Pgc1α* knockdown blocks the increase of forskolin-induced gluconeogenic genes by fascaplysin in HepG2 cells. *Pgc1α* knockdown or a negative control of HepG2 cells were treated with 30 μM forskolin and 1 μM fascaplysin overnight (one-way ANOVA with Tukey post-test, $n = 3$). **g**, *Gcn5* knockdown blunts the increase of gluconeogenic gene expression caused by *Cdk4* knockdown. Quantitative polymerase chain reaction with reverse transcription (qRT–PCR) analysis of *Pck1* and *Gcn5* and western blot of *Cdk4* and *Gcn5* knockdown are shown. All cells were infected with PGC-1α adenoviruses (one-way ANOVA with Tukey post-test, $n = 15$). **h**, PD 0332991 increases gluconeogenic genes when combined with GCN5 wild type (WT) overexpression, but not with GCN5 T272A/S372A (AA) mutant. GFP infected cells shown for comparison with GCN5 overexpressing cells. All cells were infected with PGC-1α adenoviruses (two-tailed unpaired *t*-test, $n = 6$). **i**, **j**, Insulin levels measured from serum and western blot analysis of Rb and AKT using nuclear (N) and cytoplasmic (C) liver extracts from mice treated with vehicle or 150 mg kg^{-1} PD 0332991, shown in Fig. 2l, m (**i**: two-tailed unpaired *t*-test, $n = 18$/GFP, $n = 17$/PD 0332991). **k**, Levels of cyclin D1 and Rb phosphorylation in GFP or cyclin D1 T286A tail-vein-injected mice, shown in Fig. 2n, o. Statistical significance is represented by asterisks corresponding to $^*P < 0.05$, $^{**}P < 0.01$, $^{***}P < 0.001$. Data are shown as mean ± s.e.m.

a

Body Weight and Serum Biochemistry of Vehicle or PD 0332991 Administered Mice

	Vehicle	PD 0332991
Body Weight (g)	20.41+/−0.21	20.25+/−0.27
ALT (U l^{-1})	21.46+/−2.06	16.60+/−1.58
AST (U l^{-1})	60.14+/−9.78	87.88+/−5.67
LDH (IU l^{-1})	137.80+/−3.45	176.65+/−7.63
Creatine Kinase (U l^{-1})	143.84+/−17.01	168.04+/−7.47
Total Bilirubin (mg dl^{-1})	0.77+/−0.14	0.58+/−0.18

b

Body Weight and Serum Biochemistry of GFP or Cyclin D1 T286A Injected Mice

	GFP	Cyclin D1 T286A
Body Weight (g)	20.53+/−0.24	20.51+/−0.24
ALT (U l^{-1})	9.39+/−2.45	12.88+/−2.50
AST (U l^{-1})	57.42+/−12.02	54.32+/−7.65
LDH (IU l^{-1})	90.92+/−7.51	105.78+/−2.73
Creatine Kinase (U l^{-1})	193.99+/−31.54	190.38+/−24.26
Total Bilirubin (mg dl^{-1})	0.82+/−0.40	0.39+/−0.18

Extended Data Figure 4 | PD 0332991 administration or cyclin D1 T286A adenoviral overexpression does not cause toxicity compared with its respective control treatment. **a**, Basal physiological indexes of mice challenged with either vehicle or PD 0332991 administration ($n = 5$). **b**, Basal physiological indexes of mice injected with either GFP or cyclin D1 T286A adenoviruses ($n = 5$). (ALT, alanine transaminase; AST, aspartate transaminase; LDH, lactate dehydrogenase; mean ± s.e.m.).

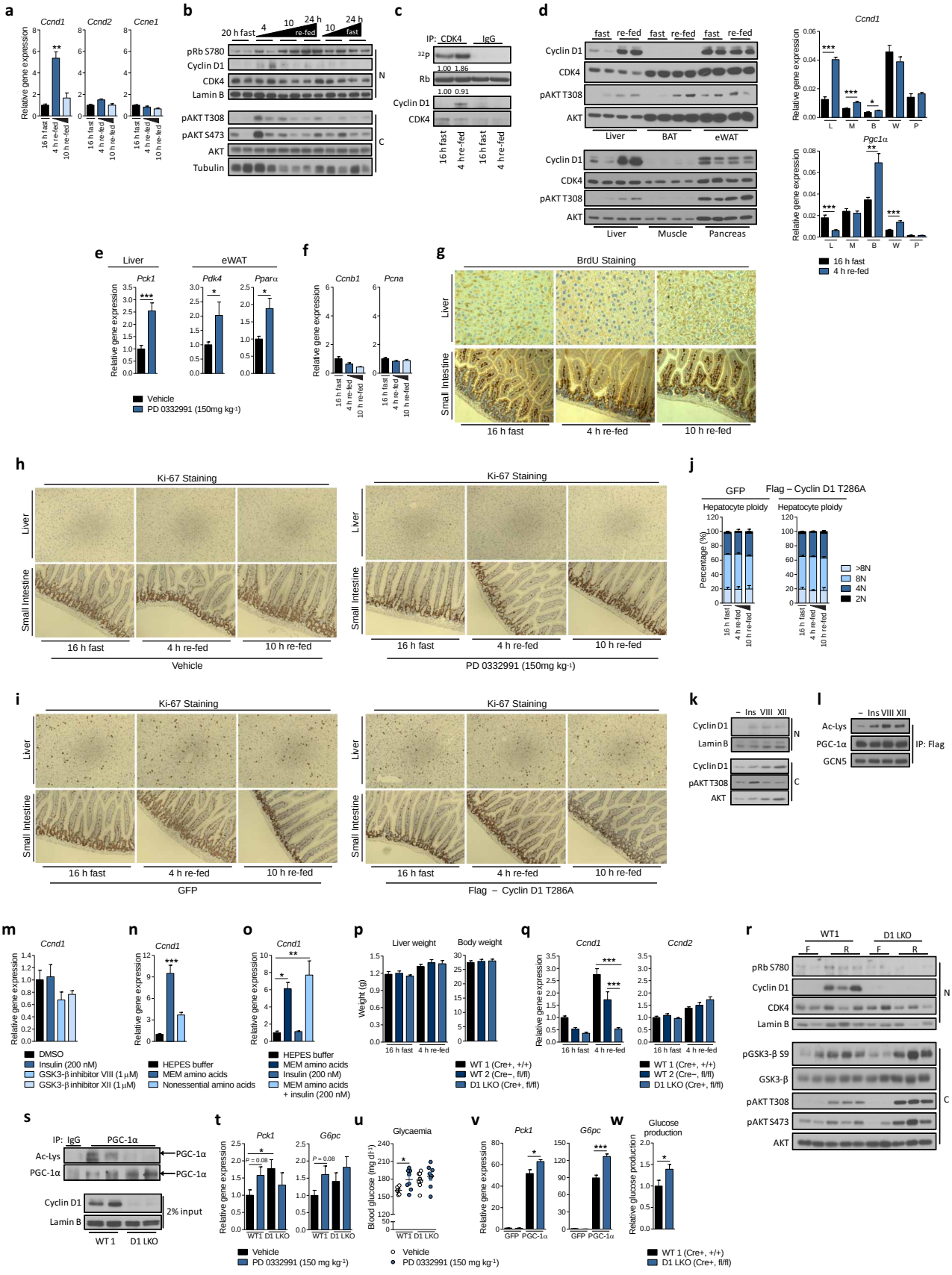

Extended Data Figure 5 | Cyclin D1–Cdk4 is regulated by insulin/GSK-3β, and hepatic specific cyclin D1 deletion causes increased gluconeogenesis and glycaemia upon re-feeding. **a**, Cyclin D1 transcripts are increased upon re-feeding. qRT–PCR analysis of *Ccnd1*, *Ccnd2* and *Ccne1* gene expression upon overnight fasting, 4 h and 10 h re-feeding in BALB/c mice livers (one-way ANOVA with Tukey post-test, $n = 3$). **b**, Cyclin D1 protein is increased upon re-feeding. Western blot analysis of cyclin D1 protein levels and associated signalling pathway upon fasting and re-feeding measured from nuclear (N) and cytoplasmic (C) liver extracts from BALB/c mice. **c**, Cyclin D1–Cdk4 kinase activity is increased upon 4 h re-feding. *In vitro* ^{32}P incorporation into recombinant Rb by immunoprecipitated cyclin D1–Cdk4 kinase from whole-cell extracts of overnight fast and 4 h re-fed livers. **d**, Western blot analysis of cyclin D1 protein level and associated signalling pathway upon fasting and re-feeding and qRT–PCR analysis of *Ccnd1* and *Pgc1α* mRNA level in various tissues (L, liver; M, skeletal muscle; B, brown adipose tissue; W, epididymal white adipose tissue; P, pancreas; two-tailed unpaired *t*-test, $n = 12$/L, $n = 4$/M, B, W, P). **e**, qRT–PCR analysis of PGC-1α target genes in liver and epididymal white adipose tissues (eWAT) upon vehicle or PD 0332991 treatment (two-tailed unpaired *t*-test, $n = 10$). **f**, *Ccnb1* and *Pcna* gene expressions in liver do not change upon fasting and re-feeding ($n = 3$/fast and 10 h re-fed, $n = 4$/4 h re-fed). **g**, BrdU incorporation in liver does not change upon fasting and re-feeding. Small intestine was used as a positive control. **h**, Ki-67 staining in liver does not change upon fasting and re-feeding after vehicle or PD 0332991 administration. The small intestine was used as a positive control. **i**, Ki-67 staining in liver does not change upon fasting and re-feeding following GFP or cyclin D1 T286A tail-vein injection. Small intestine used as a positive control. **j**, Hepatic ploidy profiles of livers of GFP or cyclin D1 T286A adenovirus tail-vein injected mice do not show significant difference. Ploidy analysis of primary hepatocytes isolated from livers measured by propidium iodide staining and flow cytometry ($n = 6$/fast and 4 h re-fed, $n = 4$/10 h re-fed). **k**, Western blot analysis of endogenous nuclear (N) and cytoplasmic (C) cyclin D1 protein level upon insulin or GSK-3β inhibitors treatments in primary hepatocytes. **l**, PGC-1α acetylation is increased upon insulin or GSK-3β inhibitors treatment in primary hepatocytes. **m**, No effect of insulin or GSK-3β inhibitors on cyclin D1 mRNA level ($n = 3$). **n**, Minimum essential medium (MEM) amino acid addition increases cyclin D1 mRNA in primary hepatocytes (one-way ANOVA with Tukey post-test, $n = 3$). **o**, Insulin does not change *Ccnd1* mRNA in primary hepatocytes (one-way ANOVA with Tukey post-test, $n = 3$). **p**, **q**, Body and liver weights and *Ccnd1* and *Ccnd2* gene expression of wild-type and liver-specific cyclin D1 LKO mice (combined four cohorts of $n = 3$/fasting, $n = 5$/re-feeding). **r**, Western blot analysis of cyclin D1 protein levels and associated signalling pathway by using nuclear and cytoplasmic liver extracts from wild-type and D1 LKO mice upon fasting (F) and 4 h re-feeding (R). **s**, Endogenous acetylation of PGC-1α is decreased in livers of D1 LKO mice compared with wild-type mice. Western blot analysis of acetylation of PGC-1α immunoprecipitated from liver nuclear extracts. All mice were killed upon 4 h re-feeding. **t**, **u**, PD 0332991 increases glycaemia with a similar tendency for gluconeogenic gene expression only in wild-type mice, but not in D1 LKO mice (two-tailed unpaired *t*-test, $n = 8$, except $n = 6$ for vehicle treated wild-type mice). **v**, **w**, Gluconeogenic gene expression and hepatic glucose production are increased in primary hepatocytes isolated from D1 LKO mice (**v**: one-way ANOVA Tukey post-test, $n = 3$; **w**: two-tailed unpaired test, $n = 6$). Statistical significance is represented by asterisks corresponding to $^{*}P < 0.05$, $^{**}P < 0.01$, $^{***}P < 0.001$. Data are shown as mean ± s.e.m.

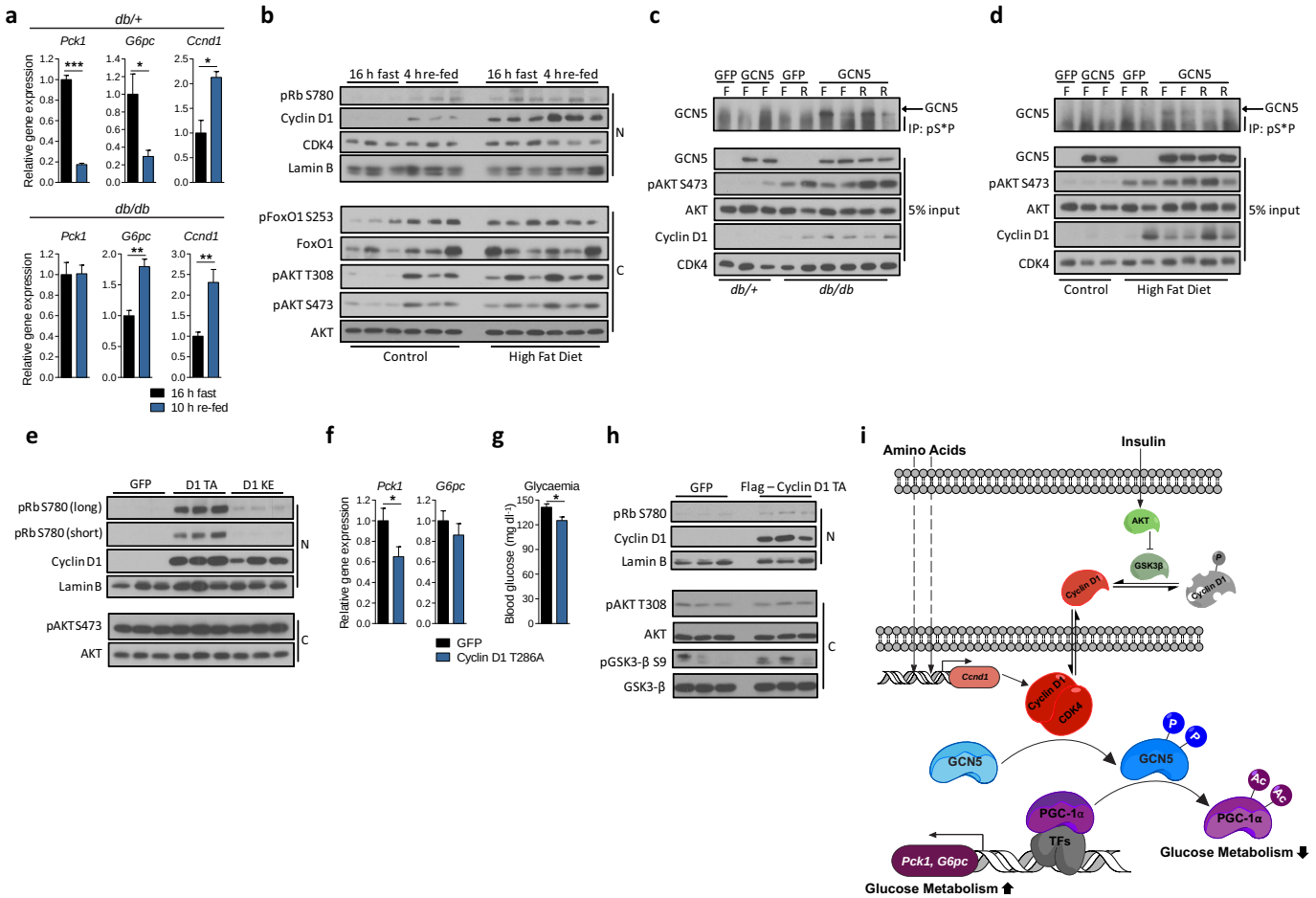

Extended Data Figure 6 | In diabetic hyperinsulinemic mice, cyclin D1–Cdk4 is dysregulated and hyperactivation of cyclin D1–Cdk4 attenuates the diabetic phenotype. **a**, qRT–PCR analysis of gluconeogenic and *Ccnd1* gene expression changes upon fasting and re-feeding in $Lepr^{db/+}$ *(db/+)* and $Lepr^{db/db}$ *(db/db)* mice livers (two-tailed unpaired *t*-test, $n = 3$). **b**, Cyclin D1 protein is chronically elevated upon fasting and re-feeding in livers of mice fed a high-fat diet compared with control diet fed mice. Nuclear (N) and cytoplasmic (C) liver extracts were used. **c**, **d**, Phosphorylation of GCN5 is elevated upon fasting in *db/db* of livers of mice fed a high-fat diet (HFD) compared with respective control mice and remains insensitive to fast–re-fed transitions. Western blot analysis of GCN5 immunoprecipitated by anti-phosphoS*P (pS*P) antibody using liver extracts from mice that were tail-vein injected with adenoviruses expressing GFP or GCN5 (F, 16 h fast; R, 4 h re-fed). **e**, Cyclin D1 and Rb phosphorylation levels in livers from *db/db* mice tail-vein injected with GFP, cyclin D1 T286A or cyclin D1 K112E adenoviruses, shown in Fig. 4b, c. Nuclear and cytoplasmic liver extracts were used. **f**, **g**, Cyclin D1 T286A overexpression reduces gluconeogenic genes and glycaemia in mice fed a high-fat diet (two-tailed unpaired *t*-test, $n = 6$/GFP, $n = 7$/D1 T286A). **h**, Cyclin D1 and Rb phosphorylation levels in livers of mice fed a high-fat diet that were tail-vein injected with adenoviruses expressing GFP or cyclin D1 T286A, shown in Extended Data Fig. 4f, g. **i**, Overall model. Statistical significance is represented by asterisks corresponding to $*P < 0.05$, $**P < 0.01$, $***P < 0.001$. Data are shown as mean ± s.e.m.